

Electron-Irradiation and Photo-Excitation Darkening and Bleaching of Yb Doped Silica Fibers: Comparison

Alexander V. Kir'yanov

Centro de Investigaciones en Optica, Leon, Mexico

E-mail: kiryanov@cio.mx

Received September 25, 2011; revised October 28, 2011; accepted November 10, 2011

Abstract

We report a comparative experimental study of the attenuation spectra transformations for a series of Yb doped alumino-germano silicate fibers with different contents of Yb³⁺ dopants, which arise as the result of irradiation either by a beam of high-energy electrons or by resonant (into the 977 nm absorption peak of Yb³⁺ ions) optical pumping. The experimental data obtained reveal that in the two circumstances, substantial and complex but different in appearance changes occur within the resonant absorption band of Yb³⁺ ions and in the off-resonance background loss of the fibers. Possible mechanisms responsible for these spectral changes are discussed.

Keywords: Ytterbium Doped Silica Fibers, Photodarkening, Electron Irradiation

1. Introduction

Yb³⁺ doped silica fibers (YFs) with different core glass hosts co-doped with aluminum, germanium, or phosphorous have been of considerable interest during the past decades as extremely effective media for fiber lasers for the spectral region 1.0 - 1.1 μm when pumped at 0.9 - 1.0 μm wavelengths. A variety of diode-pumping configurations (core and cladding) and pump wavelengths were extensively examined so far which resulted in recognition of optimal arrangements for multi-watt release from YF based lasers with high optical efficiency ~70 - 75% and perfect beam quality [1,2]. However, in spite of remarkable progress in the field, there remain certain obstacles that limit the performance of YF based lasers, one of them being the photodarkening (PD) effect [3], *i.e.* long-term (minutes to hours) degradation of laser power from units to tens %. This hardly mitigated disadvantage becomes notable when dealing with a laser based on heavily-doped YF where high Yb³⁺ population inversion is created, either at high-power continuous-wave or moderate-power pulsed lasing. A number of studies during the past years were aimed to understand the PD phenomenon which has remained unclear, although a few hypotheses have been proposed for its explanation [4-12]. Meanwhile, on one hand, the characterization procedures have been specified to quantify the PD phenomenon in YFs [9,10], allowing a proper choice among YFs for a

certain application. And on the other hand, some ways to enhance resistance of YFs to PD or at least to minimize its consequences have been suggested [13,14].

In the meantime, a few studies aimed at the characterization of susceptibility of YFs having different chemical compositions under such irradiations as x-rays, γ quanta, and UV have been reported recently [15-17]. The main motivation for these works was an inspection of resistance of YF employed in telecommunications and space technologies to harmful environments. In many cases, the excess loss spectra induced in YFs resemble the ones, characteristic for PD at resonant pumping into Yb³⁺ resonant-absorption (0.9 μm - 1.0 μm) band. This interesting fact undoubtedly deserves attention and verification by an experiment where YF would be subjected to other types of irradiation (say, by high-energy electrons) and the result of this be directly compared with the PD consequences in the same YF.

Here we report on two sets of experiments where susceptibility of YFs with similar alumino-germano (Al,Ge) silicate glass core but with different Yb³⁺ ions' concentrations is inspected under irradiation either by an electron beam or by resonant (into Yb³⁺ resonant band) optical pumping. For both circumstances, qualitatively similar trends are revealed: Strong and monotonous changes in attenuation loss of the fibers in VIS (darkening) accompanied by more complex transformations (an initial decrease followed by increase) within the resonant ab-

sorption band of Yb^{3+} ions upon dose (the case of electron irradiation) or time (the case of optical pumping at 977-nm wavelength). However, these trends are shown to be peculiar in details. Below, we compare and discuss the experimental data obtained and propose preliminary explanations.

2. Experimental Arrangement

2.1. Fibers Characterization

YFs inspected in these experiments were drawn from Al,Ge co-doped silicate glass preforms fabricated using the MCVD and solution-doping processes. The attenuation spectra in a pristine (as-received) state of the fibers are shown in **Figure 1(a)**. The concentrations of Yb^{3+} ions through a set of these YFs differed by more than an order of magnitude, so there were expected differences in the consequences of electron irradiation (further-e-irradiation) and optical pumping at 977 nm wavelength (further-OP) on the fibers' posterior properties. The fiber samples, having correspondingly the lowest, the intermediate, and the highest Yb^{3+} doping level, are referred further to as *YF-1*, *YF-2*, and *YF-3*.

2.2. Experimental Methods

A controllable linear accelerator of the LU type which sources mono-energetic (~ 6 MeV) electrons was used in experiments where a pulsed (~ 5 - μs) e-irradiation mode has been realized. The experiments were conducted at room temperature. YF samples were irradiated by placing them in the accelerator chamber during various time intervals, which provided growing irradiation doses. In-

stances "1", "2", and "3" label, on some of the figures below, doses 2×10^{12} , 1×10^{13} , and 5×10^{13} cm^{-2} , respectively. The irradiated fibers were leaved for 10 days in advance to the measurements to avoid possible short-living instabilities in the host glass, known for the fibers containing Al and Ge. Notice that ionization, *i.e.* the production of irradiation-excited carriers by an electron beam within a fiber's volume, plays the main role in the spectral transformations being reported. This is because high-energy primary electrons are virtually non-dissipating at the propagation through the fibers with an outer diameter of 125 μm . Meanwhile, some contribution in ionization might be produced by γ -quanta born at inelastic scattering of high-energy electrons propagating through the host glass.

Experiments on OP of YF at 977 nm were made by a similar way as described in Ref. [8]. YF samples were pumped using a standard 300 mW 977 nm laser diode (LD). The pump light was launched from the LD to SMF-28 fiber through a splice and then through one more splice to an YF sample. The end of the latter was spliced to another piece of SMF-28 fiber that was connected to an optical spectrum analyzer (OSA) for the transmission spectra measurements. In these experiments, we dealt with short pieces of YFs, of a cm range, to ensure no-lasing conditions and negligible contribution of amplified spontaneous emission of Yb^{3+} .

The optical transmission spectra of the YF samples were obtained using a white-light source with a fiber output and the OSA turned to a 1 nm resolution. These spectra were recorded for a spectral range 400 nm - 1200 nm, where the most interesting spectral transformations occur as the result of e-irradiation or OP. The output of the white-light source was spliced to a fiber set containing

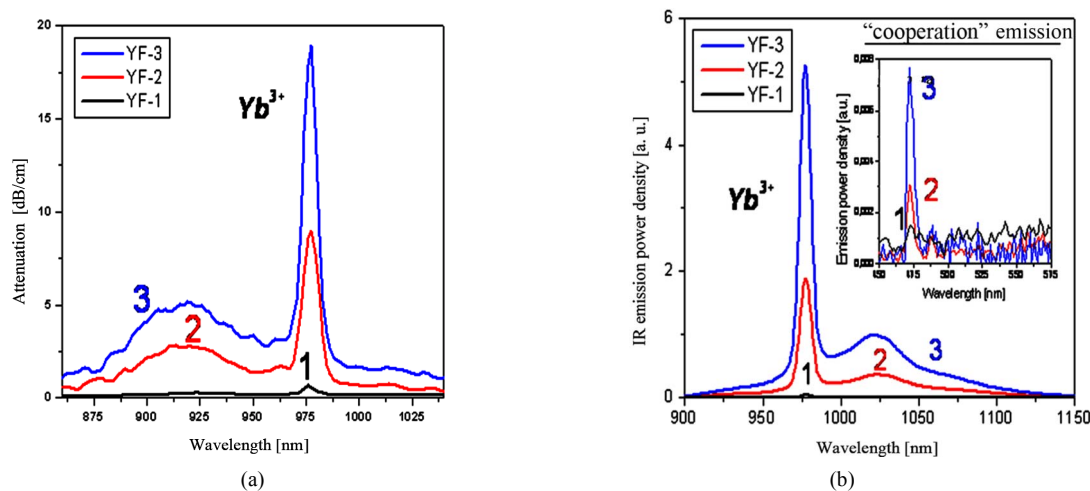


Figure 1. (a) Attenuation (small-signal absorption) spectra of fibers with low (YF-1), intermediate (YF-2), and high (YF-3) Yb^{3+} contents: curves 1, 2, and 3, respectively; (b) Fluorescence spectra of the fibers at resonant 977 nm excitation (pump power—300 mW). Labeling of curves 1, 2, and 3 is the same as in figure (a). Inset in figure (b) shows "cooperative" fluorescence in VIS.

an YF sample (pristine or subjected to e-irradiation or to OP) and white-light attenuation within the sample was recorded using the OSA. The attenuation spectra were recorded before (using pristine samples) and after each stage of e-irradiation (“doses”) or OP at 977 nm pumping (“times”). Lengths of the fiber samples were chosen to be short enough, from less than 1 cm (YF-3) to tens of cm (YF-1), to provide the final spectra free of spectral noise artifacts. We measured the attenuation spectra from VIS to near-IR, *i.e.* within the range where the main spectral transformations resulting from e-irradiation or OP occur. In some of the figures below, the difference spectra are demonstrated which were obtained after subtraction of the attenuation spectra of pristine samples from the ones taken after some dose (time) of e-irradiation (OP). This allows insight to the net spectral loss resulting from the fibers darkening. All the spectra presented below have been obtained after formal recalculating transmission coefficients in losses [dB/cm].

We also measured fluorescence spectra and fluorescence kinetics of Yb^{3+} before and after e-irradiation or after OP of the fibers, applying the lateral detecting geometry [18]. Fluorescence emission was collected from surface of an YF sample at the point spaced by approximately 5 mm from its splice with an output fiber of the LD. We used the same OSA for the fluorescence spectra measurements and a Ge photo-detector and oscilloscope for the fluorescence decay measurements. In the last case, LD power was modulated by a driver controlled by a function generator’s signal to achieve square-shaped pulses with sharp rise and fall edges. The time resolution of the entire experimental setup was approximately 8 μs .

3. Experimental Results

3.1. E-irradiation experiments

The results of these experiments are highlighted by **Figures 2, 3, 4(a)-(b)** and 7.

The attenuation spectra of samples YF-3 and YF-1, having correspondingly the highest and lowest Yb^{3+} concentrations, after different doses of e-irradiation along with the attenuation spectra of the samples in a pristine (dose “0”) state are shown in **Figure 2(a)-(b)**.

First, a notable increase of background loss in the fibers in VIS with increasing e-irradiation dose is revealed from **Figure 2** (see main frames). Also notice a specific spectral character of this loss for both fibers, that is, a drastic rise of its magnitude towards shorter wavelengths. This is a trend well-known for the experiments on influence of various-type irradiations upon optical properties of Yb^{3+} -free silica fibers. At the same time, the apparent differences are seen in magnitude of e-irradiation induced loss in these two samples, *i.e.* a much higher level of darkening in YF-3 than in YF-1. [The data for sample YF-2, intermediate in Yb^{3+} doping level, demonstrate similar but intermediate growth of the background loss in VIS as compared to samples YF-3 and YF-1.]

Second, definitive but less pronounced spectral transformations are revealed for the resonant-absorption band of Yb^{3+} (850 - 1100 nm); see insets to **Figures 2(a)-(b)**. The insets show the difference spectra obtained as it is described in Section 2. Vastly small in sample YF-1 (**Figure 2(b)**), the spectral transformations become significant in sample YF-3 (**Figure 2(a)**) and they have a complex

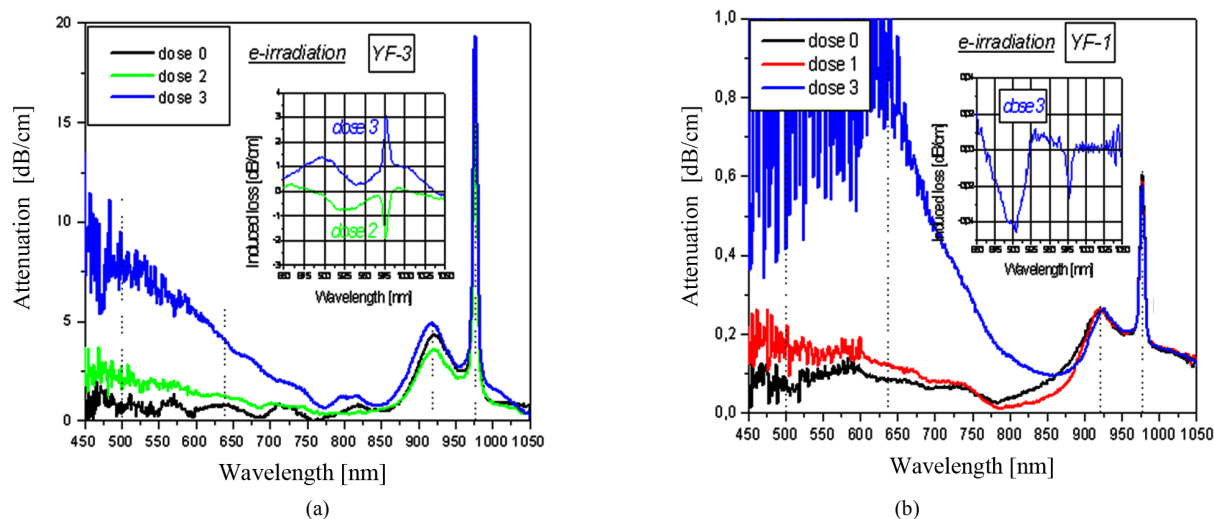


Figure 2. Attenuation spectra of samples YF-3 (a) and YF-1 (b). The data are for e-irradiation doses increased from “0” (pristine samples) through “1” and “2” to “3”. Insets show the difference spectra obtained after subtraction of the spectra of pristine samples from the ones after e-irradiation of the samples. Dashed lines schematically show the positions of wavelengths for which the data in Figure 3 are built.

character regarding e-irradiation dose growth: Compare the difference spectra obtained after doses “2” and “3”. The revealed behavior seems to be a consequence of some process associated with e-irradiation which affects the concentration of Yb^{3+} ions.

More details are seen from **Figure 3** where we plot the results obtained for samples YF-1 (a) and YF-3 (b), taken from the whole set of e-irradiation doses. **Figures 3 (a)-(b)** demonstrates how attenuation within the resonant-absorption of Yb^{3+} (peaks at 920 and 977 nm, see also **Figure 1(a)**) changes through e-irradiation: See curves 1 (for the 977 nm peak) and curves 2 (for the 920-nm peak), respectively. A decrease followed by increase of the magnitude of small-signal absorption coefficient arises in both peaks with increasing e-irradiation dose in YF-3 (heavier doped with Yb^{3+}); notice that this behavior is much less expressed in YF-1 (lower doped with Yb^{3+}).

For comparison purposes, we also plot in **Figure 3** the changes in attenuation of samples YF-3 (c) and YF-1 (d)

in VIS where background (non-resonant) losses arise as the result of e-irradiation. Here we limit ourselves by giving the data for a couple of wavelengths in VIS, at 500 (curve 3) and 633 (curve 4) nm. It is seen that background loss monotonously (almost linearly) grows with e-irradiation dose, a common effect for silica based fibers. Importantly, the rate of growth is higher in YF-3 than in YF-1. Furthermore, it deserves attention that an initial level of background loss in pristine YF samples correlates with an initial content of Yb^{3+} ions. [The data for sample YF-2 are similar to the ones shown in **Figure 3** for samples YF-3 and YF-1, but the magnitude of spectral transformations in YF-2 is intermediate when comparing those in YF-3 and YF-1.]

In **Figures 4(a)** and **(b)**, we gather the experimental results from **Figures 2** and **3** for samples YF-1 and YF-3 and add the data for sample YF-2. This allows seeking the concentration dependences of the resonant (Yb^{3+}) and background loss induced in the fibers at e-irradiation upon

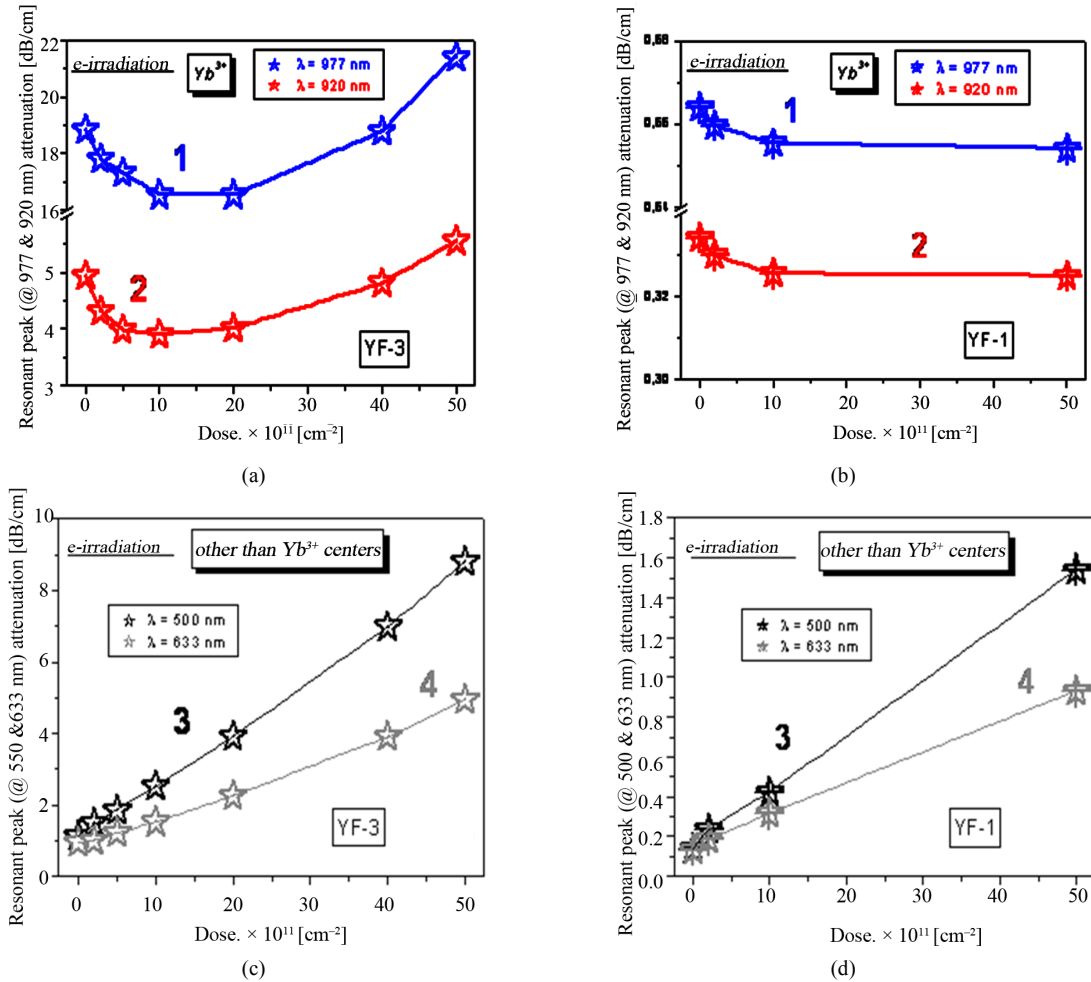


Figure 3. Dose dependences of attenuation in resonant-absorption Yb^{3+} peaks centered at 977 (curves 1) and 920 (curves 2) nm (top panels) and in VIS, for wavelengths 500 (curves 3) and 633 (curves 4) nm (bottom panels). The data are for samples YF-3 (a, c) and YF-1 (b, d).

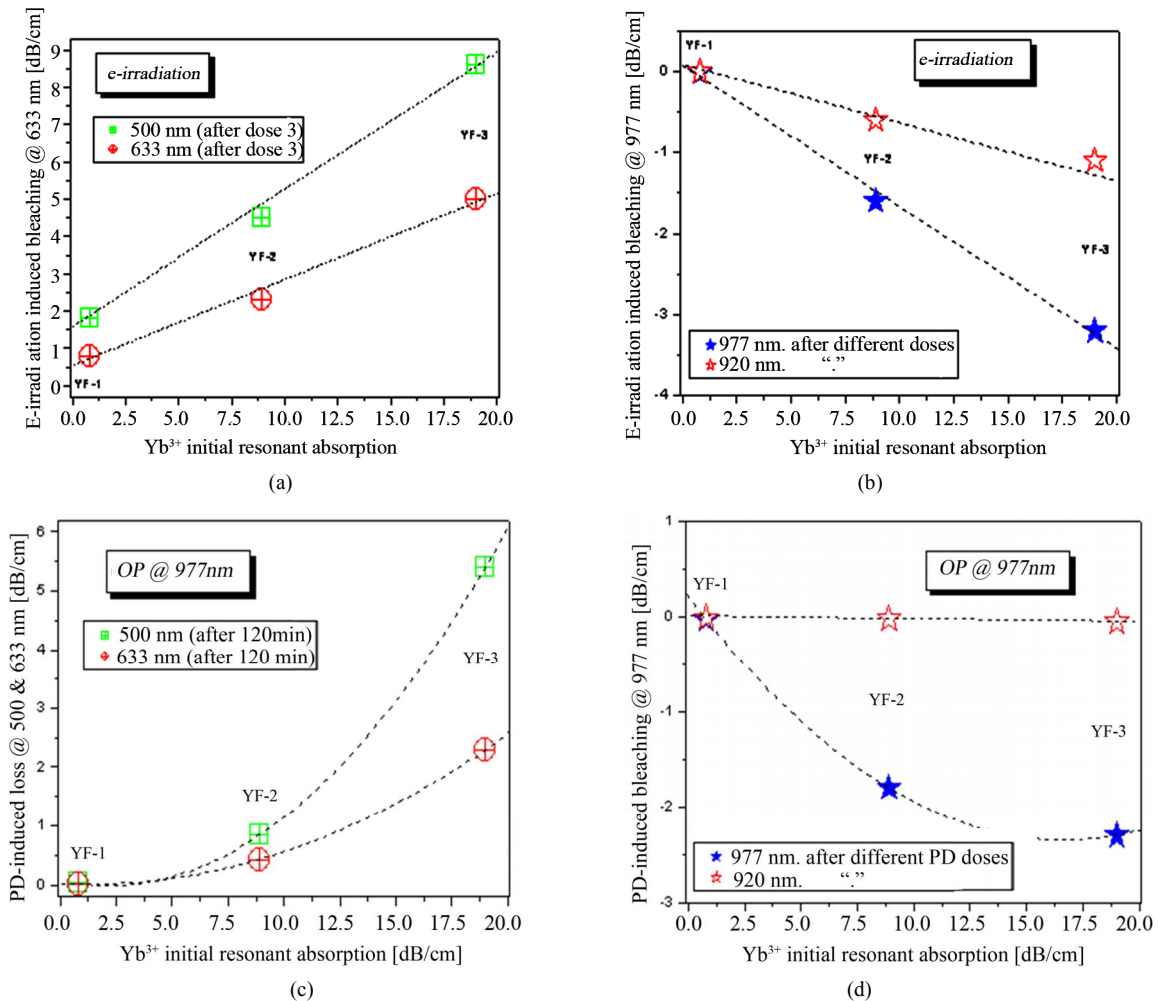


Figure 4. The results of experiments with fibers YF-1, YF-2, and YF-3, which were obtained for different e-irradiation doses (a, b) and OP times (c, d). The data are for the resonant-absorption peaks at 977 and 920 nm (filled and empty asterisks) (b, d) and for the VIS region, exemplified by wavelengths 500 nm (crossed squares) and 633 nm (crossed circles) (a, c). Dotted lines are for visual purposes only.

the value of small-signal absorption coefficient at 977 nm. From **Figure 4(a)**, one can first reveal a monotonic increase of background (non-resonant) loss in VIS (darkening), exemplified by wavelengths 500 and 633 nm, with increasing Yb³⁺ concentration, in turn proportional to YF small-signal absorption at 977 nm. This demonstrates that the presence of Yb³⁺ dopants in the fibers gains their degradation at e-irradiation. Here we show the results obtained for e-irradiation dose “3” only since for the other doses the dependences are similar, given by a monotonic dose dependence of the induced loss in VIS (refer e.g. to **Figures 3 (c)-(d)**).

Then, from **Figure 4(b)** it is seen that the lowest levels, to which the values of the resonant absorption in the 977 nm peak approach through e-irradiation (minima of curves 1 in **Figure 2**), decrease with increasing Yb³⁺ concentration through a set of samples YF-1, YF-2, and YF-3. A

similar trend is observed for the other peak of Yb³⁺ (at 920 nm). This fact seems to be in favor of that initial concentration of Yb³⁺ ions in pristine samples substantially decreases as the result of e-irradiation (at its primary stage). However, it should not be overlooked that at the following stages of e-irradiation Yb³⁺ concentrations are re-established on the levels comparable with those in pristine YFs (refer to **Figure 3(a)**).

The remainder of **Figure 4**, graphs (c) and (d), gives the results obtained in the experiments on spectral transformations in YFs at OP which are reported in the next sub-section.

3.2. OP experiments

The results of these experiments are highlighted by **Figures 4(c)-(d)** and **Figures 5-8**.

We limit ourselves by reporting here the results of OP experiments for sample YF-3 mainly (see **Figures 5-7** below), having the highest content of Yb^{3+} ions in a pristine state. Meanwhile, we summarize all of the results (for samples YF-1, YF-2, and YF-3) in **Figure 4(c)-(d)**.

Figure 5 shows the attenuation spectra of sample YF-3 (having a short length of 0.8 cm) after 40 and 120 min. of OP. LD power was fixed in these experiments at approximately 300 mW, providing the highest attainable level of Yb^{3+} population inversion. For comparison, the

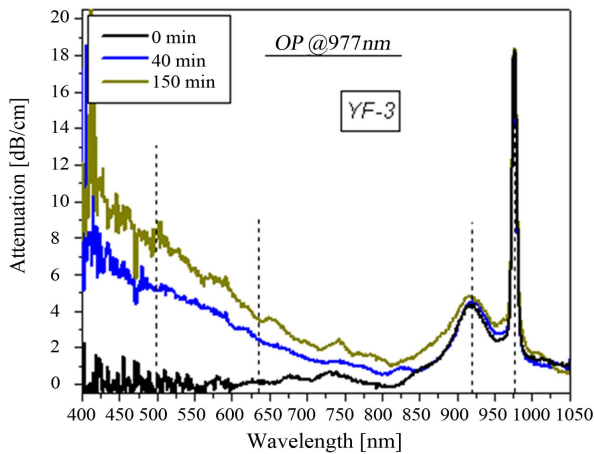


Figure 5. Attenuation (small-signal absorption) spectra of fiber sample YF-3 after OP @ 977 nm. The data are for a pristine sample (curve 1: “0 min”) and for photo darkened samples (curves 2 and 3, obtained after 40 and 150 min of OP, respectively). Dashed lines show the positions of wave-lengths for which the data in **Figure 6** are built.

attenuation spectrum of a pristine (0 min) sample YF-3 is shown in **Figure 5**, too. Once compared with the attenuation spectra after e-irradiation (refer to **Figure 2(a)**), these spectra are seen to be similar in appearance. That is, a substantial increase of background loss arises in VIS with increasing OP time (the PD effect). Notice that the spectral signature of PD resembles the one at darkening after e-irradiation (refer to **Figure 2**). The spectral changes that occur within the resonant (Yb^{3+}) absorption band at PD of are discussed below; see **Figure 7**.

In **Figure 6(a)**, we demonstrate the results of the experiments with sample YF-3, obtained at increasing OP time. Their representation is similar to the one used at the description of experiments on e-irradiation, see **Figure 3(a)**. From **Figure 6(a)**, it is seen how attenuations in the two absorption peaks of Yb^{3+} ions (at 977 and 920 nm) change through OP; see curves 1 and 2, respectively. The time dependence of OP induced changes at 977 nm resembles the dose dependence at e-irradiation of sample YF-3 (see curve 1 in **Figure 3(a)**). However, curve 1 in **Figure 6(a)** has an “asymmetric” shape versus OP time, differing from a “symmetric” shape of the dose dependence at e-irradiation given by curve 1 in **Figure 3(a)**. Furthermore, the time dependence of OP induced changes at 920 nm, see curve 2 in **Figure 6(a)**, is seen to be very weak, being completely different from curve 2 in **Figure 3(a)** (e-irradiation). Therefore, we can propose that somewhat different mechanisms are involved in these two (e-irradiation and OP) treatments of the fibers which are responsible for the induced changes within the resonant-absorption band of Yb^{3+} at 977 and 920 nm.

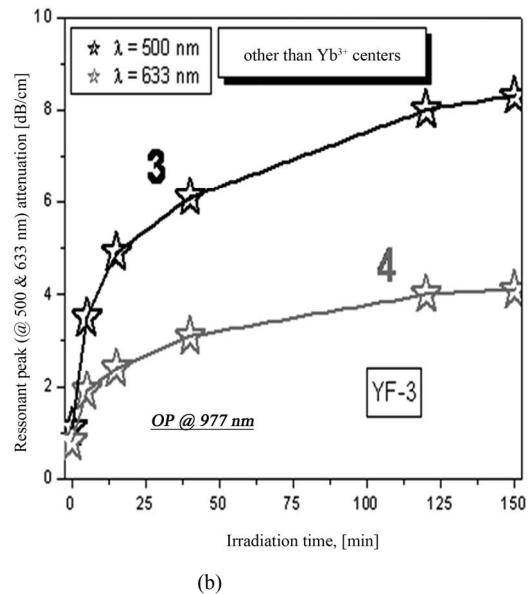
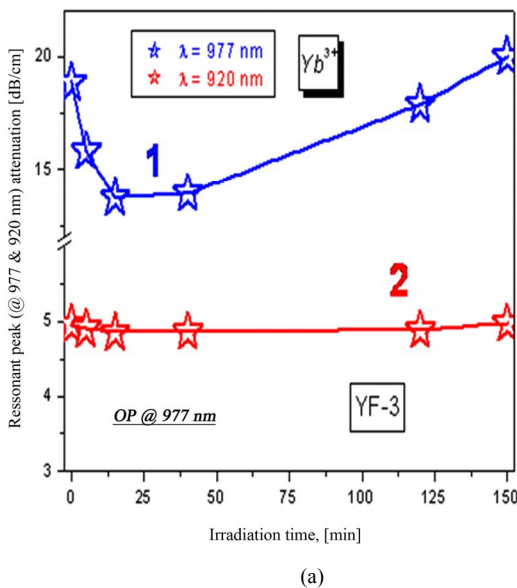


Figure 6. Dose dependences of attenuation in resonant-absorption (Yb^{3+}) peaks centered at 977 (curve 1) and 920 (curve 2) nm (a) and in VIS, for wavelengths 500 (curve 3) and 633 (curve 4) nm (b). The data are for sample YF-3.

In **Figure 6(b)**, we demonstrate the results of all of the spectral transformations that occur in sample YF-3 in VIS, where non-resonant background loss arises as the result of OP. This can be also seen by referring to **Figure 5** and compared with the results of e-irradiation shown in **Figure 3(c)**. Again, we provide in **Figure 6(b)** the data for a couple of wavelengths only, 500 (curves 3) and 633 (curves 4) nm, as the representatives. In contrast to the dose dependences at e-irradiation, long-term OP at the resonant wavelength 977 nm results in completely different dynamics of background loss with time. Indeed, it is essentially nonlinear in time: There is a short time interval in the beginning (few minutes) where PD increases dramatically while in the remainder of OP (tens of minutes) PD slows down and tends to saturate. Note that the described time dependences are very similar to the ones commonly met at PD experiments with YFs at 633-nm probing (a He-Ne laser).

Let's now consider the results shown in **Figures 7** and **8** where we make insight to the difference spectra.

Figure 7 allows a direct comparison of the attenuation spectra for sample YF-3 after dose "3" of e-irradiation (curve 1) and after 2 hours of OP (curve 2). The spectra look qualitatively similar which could validate the mechanisms that stand behind the spectral transformations to be basically similar. At the same time, if one spectrum is formally subtracted from another, the result (curve 3 in **Figure 7**) shows a definitive difference. That is, apart from the difference in the background loss which ought to be present in anyway, there is a feature within the Yb^{3+} resonant band: Although no deviation from a "plain" behavior of curve 3 is seen nearby 920 nm peak of Yb^{3+} , there is a well-pronounced 977 nm

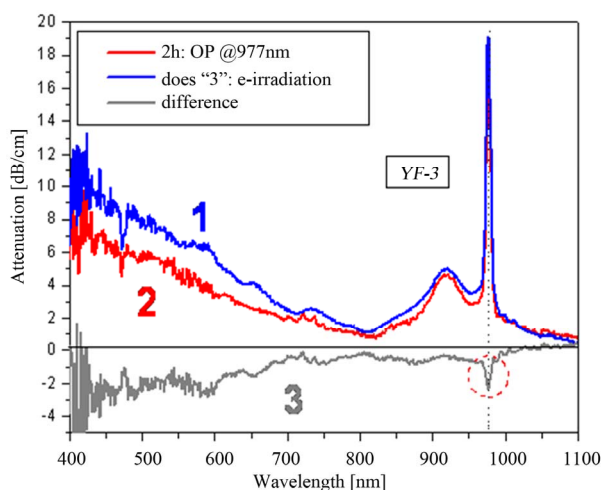


Figure 7. Difference attenuation spectra after dose "3" of e-irradiation (curve 1) and after 2 hours of OP at 977 nm (pump power is 300 mW) (curve 2); curve 3 is the difference of spectra 1 and 2. The data are for sample YF-3.

peak (it is marked by a dotted ring on **Figure 7**). This detail seems to be important because it lightens non-homogeneity within the Yb^{3+} resonant-absorption band nearby 977 nm, present at long-term OP but not—at e-irradiation of the fiber.

This becomes more apparent when an analysis of the results of OP-induced PD of the other samples, YF-1 and YF-2, has been made. Indeed, from **Figures 8 (a)-(b)**, where we plot the difference spectra obtained for these fibers, a firm spectral detail is seen to appear exactly within the 977 nm peak of Yb^{3+} ions (it is marked by a dotted ring in plots (a) and (b)). This fact can be interpreted as follows: At OP-induced PD, that is, at rising of background loss tailing from VIS towards near-IR (see the left part of **Figures 8(a)-(b)**), drastic decreasing of the resonant absorption occurs within a narrow 977-nm peak. Some more assertions on this feature are made in the Discussion section.

In **Figures 4(c)-(d)**, we gather the results of OP experiments for an entire set of YF samples, seeking the concentration dependences of the resonant (within the Yb^{3+} band) and background non-resonant spectral transformations.

In contrast to the results of e-irradiation (refer to **Figures 4(a)-(b)**), one can firstly reveal essentially nonlinear growth of background loss at wavelengths 500 and 633 nm with increasing Yb^{3+} concentration (**Figure 4(c)**). Obviously, it is different from linear growth of background loss at e-irradiation of the fibers (**Figure 4(a)**). Secondly, it is seen that instead of a linear decrease of resonant absorption peaks at 977 and 920 nm with dose, occurring at primary stages of e-irradiation (see **Figure 4(b)**), a strongly nonlinear law is seen to fit a decrease of the resonant absorption peak at 977 nm while almost no change to be present at 920 nm; see **Figure 4(d)**.

Hence, the situation with OP induced spectral transformations in our YFs is more complex and curious at first glance. The 977 nm peak is strongly affected by OP, not the 920 nm one. This can be explained by the presence in the fibers of centers others than Yb^{3+} dopants, but closely related to them and spectrally matching them nearby 977 nm. Moreover, partial weight of such centers in YF core ought to increase with increasing Yb^{3+} ions concentration. The nonlinear behavior of non-resonant background loss versus OP time, revealed above (see **Figure 6(b)**), seems to be a closely related phenomenon.

It should be noted that at further exposure of YFs to OP an initial state of the resonant absorption peaks tends to restore (**Figure 6(a)**), thus demonstrating the behavior quite similar to e-irradiation of the fibers (**Figure 3(a)**).

3.3. Fluorescence Measurements

The fluorescence spectra obtained for pristine samples

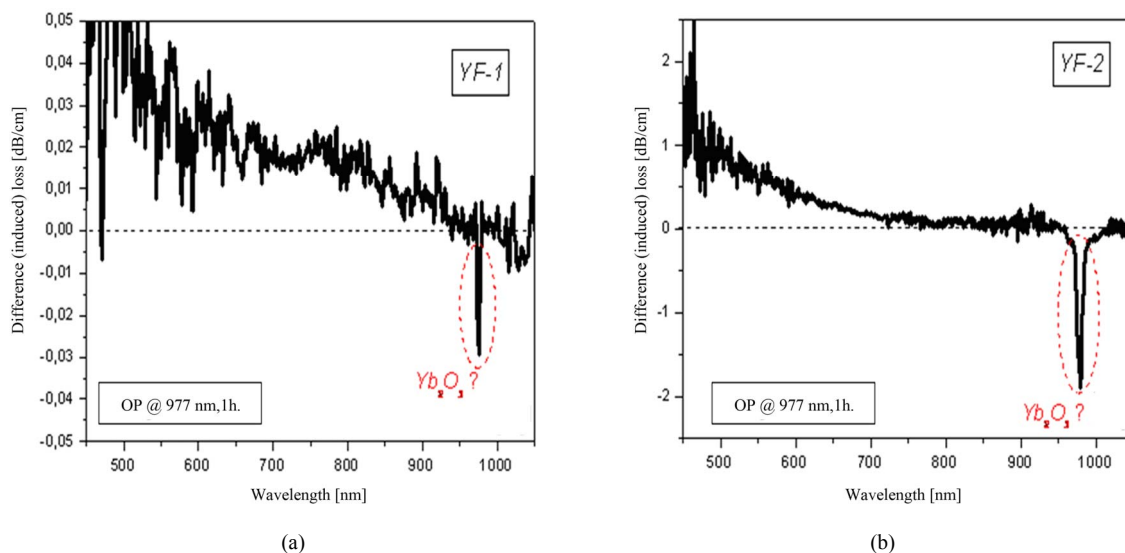


Figure 8. Difference (loss) spectra of samples YF-1 (a) and YF-2 (b), obtained after 1-hour of OP at 977 nm (pump power is 300 mW).

YF-1, YF-2, and YF-3 at 977-nm pumping are shown in **Figure 1(b)**. All of these are similar in appearance and their intensities are proportional to concentrations of Yb^{3+} in the fibers. [The measurements were made at the same conditions and for same pump powers.]

We also measured the fluorescence spectra of the fibers after irradiation by an electron beam or after long-term OP at 977 nm, but we couldn't capture any qualitative spectral change within the Yb^{3+} fluorescence band; so, we don't provide them here. We could only see a small decrease in the fluorescence intensity as the result of irradiations but obviously this trend could not be quantified.

For the fluorescence decays measured at modulated pumping of the YFs, it was found that the characteristic Yb^{3+} fluorescence decay time slightly decreases through the set of pristine YF samples. This is a result of the presence of two exponents in the fluorescence kinetics measured by ~ 0.7 ms (main) and $\sim 0.2 - 0.3$ ms ("auxiliary"). Notice that insignificant growth of the latter contribution was detected for the fiber with the highest Yb^{3+} content (YF-3); see also Refs. [18-20]. However, the time constants obtained for fitting the decays were found to be non-affected neither after e-irradiation nor after long-term OP. A lone novelty found was that both the treatments gave rise to growth of scattering in the fibers at the pump wavelength. This extra scattering looked as an instantaneous (within the resolution limit of 8 μs) drop of a signal from the photo-detector, followed by slow Yb^{3+} fluorescence decay. Since such a scattering signal was virtually not present in pristine samples, this observation might deserve attention.

Concluding, we can reveal that none, or vastly small, changes occurred with our YFs in the sense of Yb^{3+} fluorescence properties.

4. Discussion

4.1. Interpretation of Experimental Results

Summarizing all the data reported in Section 3, we notice that either at e-irradiation or at resonant OP of YFs substantial and complex but different in appearance changes arise within the resonant absorption band of Yb^{3+} ions ("reversible bleaching") while monotonous growth of non-resonant background loss occurs in VIS ("darkening"). Furthermore, these trends are revealed to originate from the changes in concentrations of Yb^{3+} ions and seemingly of other centers, closely related to them and spectrally matching them nearby 977 nm. This is the main result of our experiments. In the meantime, in virtue of importance of the details figured out above a few more assertions can be made.

A general consequence of the experiments on e-irradiation, a rise of background non-resonant loss in YFs in VIS (see **Figures 3(c)-(d)**), is not surprising. This loss correlates by a spectral signature with the excess loss that arises in optical fibers after other types of irradiation (x-rays, γ quanta, UV [15-17]). Some other aspects are as follows:

(1) A monotonic increase of the background loss in VIS (darkening) with increasing Yb^{3+} content in the YFs which demonstrates, as it was already mentioned, that the presence of Yb^{3+} dopants leads to a higher degree of

degradation of the fibers at e-irradiation; see **Figure 4(a)**;

(2) A notable decrease followed by equally notable increase that arise in the resonant-absorption peaks of Yb^{3+} (at 920 and 977 nm) with increasing e-irradiation dose (**Figure 3(a)-(b)**), the effect also dependent on Yb^{3+} concentration; see **Figure 4(b)**.

Thus, the presence of Yb^{3+} dopants in the fibers results in a more pronounceable degradation as the result of e-irradiation, with a probable reason being that Yb^{3+} ions are powerful sources of secondary carriers (electrons and holes) born at e-irradiation. That is, the changes within the resonant-absorption band of Yb^{3+} may stem from e-irradiation induced excitation of inner-shell (*f*) electrons of Yb^{3+} and their valence transformation through the charge-transfer (CT) processes (direct and return), sketched by the following reactions [8,21]: $e^- + \text{Yb}^{3+} \rightarrow \text{Yb}^{2+}$; $e^+ + \text{Yb}^{2+} \rightarrow \text{Yb}^{3+}$, where e^- and e^+ are the notations for secondary (irradiation induced) electrons and holes and Yb^{2+} is the notation for Ytterbium ions in valence-two state. In turn, the presence in the fibers of secondary carriers as the result of e-irradiation can cause formation of such defects as oxygen-deficit (ODC) and non-bridging oxygen-hole (NBOHC) centers [19,22]. These centers are known to be responsible for the wide excess-loss spectral bands similar to the ones formed in our darkened fibers; see **Figures 2 and 7**.

(2) Qualitatively similar observations can be made regarding the spectral transformations in the YFs as the result of OP at 977 nm; refer to **Figures 4(c)-(d)** and **Figures 5-8**.

Analogously, the following trends are revealed:

(3) Background loss in VIS significantly grows at long-term OP (see **Figures 5 and 6(b)**) and its character is typical for the PD effect in YFs [3-13]. At the same time, an increase of this loss in VIS with increasing small-signal absorption has, in contrast to e-irradiation, a strongly nonlinear law (see **Figure 4(c)**), thus revealing an almost quadratic dependence versus Yb^{3+} concentration in the fibers [23];

(4) The dependences of resonant absorption, measured in the peaks of Yb^{3+} at 977 and 920 nm upon OP time, have essentially different characters (see **Figure 6(a)**). If the absorption coefficient in the 977 nm peak changes by a law similar to the one at e-irradiation (a primary decrease followed by increase versus time), the absorption coefficient in the 920 nm peak is virtually constant through long-term OP. The concentration dependences shown in **Figure 4(d)** tell us more: The changes in these peaks with increasing content of Yb^{3+} ions in the fibers are also different. We cannot interpret these details in terms of simple concentration dependences with regard to Yb^{3+} ions. Otherwise, an assumption should be made instead that the changes in the 977 nm peak are related to

the changes in concentration of some centers others than Yb^{3+} ions but spectrally matching them nearby the 977 nm peak;

(5) The spectral signature of the latter is seen from **Figures 7 and 8** where the difference attenuation spectra after OP are presented. One can capture from **Figures 7 and 8** that the PD effect (growth of non-resonant loss in VIS) is accompanied by bleaching of the resonant peak at 977 nm whereas none occurs with the peak at 920 nm. Notice that a similar feature was reported earlier for other type of YF, fabricated by the DND method [8].

All the facts (3-5) being gathered together, tell us that PD in YF at high-power long-term OP at 977 nm occurs among the centers the concentration of which is a non-linear (almost quadratic) function of Yb^{3+} ions concentration. These are most probably the centers composed of couples of Yb^{3+} ions ("pairs"). Furthermore, similar reactions: $e^- + \text{Yb}_p^{3+} \rightarrow \text{Yb}_p^{2+}$; $e^+ + \text{Yb}_p^{2+} \rightarrow \text{Yb}_p^{3+}$ (see above) can be written to address these transformations at OP, where index *p* stands to emphasize that a pair of Yb^{3+} ions is involved in the processes and notations e^- and e^+ are used for an electron and hole, free or trapped by the nearest ligand, say oxygen [8,24]. Such reactions can also go at the assistance of CT processes between ion pairs where both the constituents are in the excited state. Hence, the spectrally wide background loss (PD) in the fibers, see **Figures 5 and 7**, can stem from producing of Yb_p^{2+} and of e^-/e^+ -related centers (say, ODC and NBOHC) at OP like this takes place at e-irradiation.

It is currently believed that PD occurs among clusters of Yb^{3+} ions (obviously, pairs are their kind). However, a meaningful novelty found in the present study for the first time is the spectral feature, occurring at OP (see dotted rings in **Figures 7 and 8** but not - at e-irradiation).

4.2. Pre-concluding Remarks

There are evidences for that the PD process can be associated with non-binding oxygen near surfaces of Yb/Al clusters that can be formed in alumino-silicate glass (our case). The non-binding oxygen originates from Yb^{3+} substituting Si^{4+} sites. When subjecting an YF to 977-nm OP, the excess energy is radiated as phonons, causing a lone electron of a non-binding oxygen atom to shift to a nearest neighbour non-binding oxygen atom with creation of a hole and a pair of lone electrons, which results in a Coulomb field between the oxygen atoms to form an unstable "color" center. The conversion of such an unstable center to a semi-stable center requires the shifting of one electron of the lone electron pair to a nearest neighbour site [25]. As a result of this, the formation of Yb- (and probably Al-) related ODC can occur. On the other hand, PD in alumino-silicate YFs may take place

through the breaking of ODC, which gives rise to release of free electrons. The released electrons may be trapped at Al or Yb sites to form a color center resulting in PD. These hypotheses can serve as the arguments, bringing more clarity in understanding of similarity of the spectral transformations in YFs at e-irradiation (creation of “secondary” carriers in the core glass by an electron beam) and at OP (creation of carriers and color centers by the pump light).

II. Some more assumptions can be made in attempt to understand the PD phenomenon at OP. Of course, different “paired” complexes (say, Yb-O-Yb or more complicate clusters of such kind) can be thought to be involved at PD, but we suggest here Yb₂O₃ “molecules” (or their agglomerates), the presence of which in YFs at increasing Yb³⁺ ions concentration is quite probabilistic [26]. It is also worth noting that CT transitions are well-known for Yb-doped sesquioxides (Yb₂O₃ is one of them) while these are still debated for single Yb³⁺ ions “dissolved” in YF core glass [8,12,27,28]. So, Yb_p³⁺ in the form of inherent centers Yb₂O₃, absorption spectrum of which matches well the spectral feature ringed in **Figure 8**, seem to be relevant candidates to explain PD: Refer e.g. to the works [29,30] where the presence of the strong 977 nm peak and the absence (vanishing) of the 920-nm peak was revealed to be characteristic for Yb₂O₃ (see also Ref. [31] where the peaks at 977 nm from single and paired Yb³⁺ are shown to match spectrally). Furthermore, on one hand, the presence of cooperative VIS fluorescence at 977 nm excitation (see inset in **Figure 1(b)**) is typical for Yb₂O₃ [32], while on the other hand, PD was proved to be associated with the presence of cooperative processes in YFs [7,33]. (The spectral feature seen in **Figure 1(b)** in VIS is undoubtedly ascribed by us to the cooperative fluorescence of Yb³⁺ since no other spectral features were detected which would originate from traces of un-wanted rare-earth dopants [34,35] like Tm³⁺.)

One more assumption can be made that Yb₂O₃ is a typical defect center in the core glass network which can be formed at high Yb³⁺ concentrations. Probably, namely this “color” center, firstly detected yet in 1997 [36], is responsible for the presence of non-saturated (by 977-nm radiation) resonant absorption in heavily Yb³⁺ doped fibers [18,36-38]. This non-saturated absorption can be understandable in virtue of extremely high absorption coefficient at 977 nm ($\sim 1 \times 10^{20}$ cm²) and almost quenched fluorescence (~ 10 μs), characteristic for Yb₂O₃ centers [28,32,39]. Apparently, these values are completely incompatible with those known for single Yb³⁺ ions dissolved in the core glass: $\sim 1 \times 10^{21}$ cm² and ~ 1 ms, respectively; see e.g. Ref. [40]. Further, possible presence of Yb₂O₃ centers in heavily-doped YF, which in-

tensively absorb the pump light but are non-fluorescent (“quenched”), may cause an excessive temperature rise in YF core.

It is logical to bridge here to the papers [41,42] where the idea of an intrinsic color center, like Yb₂O₃, has been proposed to address some of the concentration phenomena in heavily rare-earth doped materials. So, the physical essences given by doping YF with Yb₂O₃ (non-intentionally or intentionally [43]) can be of importance.

III. We didn't discuss above a possible role of the spectral changes in refractive index of YFs at OP and e-irradiation which ought to be induced as well, according to the Kramers–Kroönig relations. A study of these changes can be the substance of a future work.

5. Conclusions

We report a comparative experimental study of the attenuation spectra transformations for a series of Yb doped alumino-germano silicate fibers with various Yb³⁺ contents, occurring as the result of irradiation either by a beam of high-energy electrons or at in-band optical pumping at 977 nm wavelength. Substantial and complex but different in appearance changes are found to arise within the resonant absorption band of Yb³⁺ ions (reversible bleaching) while monotonous growth of non-resonant background loss to occur in VIS (darkening). Both the trends are shown to originate from the changes in concentrations of either Yb³⁺ ions (at electron irradiation) or other centers, seemingly Yb³⁺ clusters, closely related to single Yb³⁺ ions and spectrally matching them at 977 nm (at optical pumping). So, in both cases, *i.e.* at photodarkening, observed in heavily Yb³⁺ doped fibers at resonant (977 nm) optical pumping, and at electron irradiation-induced darkening of the fibers, we can capture a notable role of Yb³⁺ dopants as the agents, creating high-energy radiation, responsible for formation of color centers in the fibers, and at the same time their role as the sensitizers of these processes.

6. Acknowledgements

Author thanks Dr. N.S. Kozlova (MISIS, Moscow, Russia) and Dr. A.D. Guzman Chavez (CIO, Leon, Mexico) for help in making e-irradiation and photodarkening measurements, respectively, and Dr. Yu.O. Barmenkov (CIO, Leon, Mexico) and Dr. N.N. Il'ichev (GPI, Moscow, Russia) for useful discussions.

7. References

- [1] H. M. Pask, R. J. Carman, D. C. Hanna, A. C. Tropper, C. J. Mackechnie, P. R. Barber and J. M. Dawes, “Ytter-

- bium-Doped Silica Fiber Lasers: Versatile Sources for the 1 - 1.2 μm Region," *IEEE Journal of Quantum Electronics*, Vol. 1, No. 1, 1995, pp. 2-13. doi:10.1109/2944.468377
- [2] D. J. Richardson, J. Nilsson and W. A. Clarkson, "High-Power Fiber Lasers: Current Status and Future Perspectives," *Journal of Optical Society of America B*, Vol. 27, No. 11, 2010, pp. B63-B92. doi:10.1364/JOSAB.27.000B63
- [3] J. J. Koponen, M. J. Soderlund, H. J. Hoffman and S. K. T. Tammela, "Measuring Photodarkening from Single-Mode Ytterbium Doped Silica Fibers," *Optics Express*, Vol. 14, No. 24, 2006, pp. 11539-11544. doi:10.1364/OE.14.011539
- [4] J. Kirchhof, S. Unger, A. Schwuchow, S. Grimm and V. Reichel, "Materials for High-Power Fiber Lasers," *Journal of Non-Crystalline Solids*, Vol. 352, No. 23-25, 2006, pp. 2399-2403. doi:10.1016/j.jnoncrysol.2006.02.061
- [5] I. Manek-Honninger, J. Boulet, T. Cardinal, F. Guillen, M. Podgorski, R. Bello Doua and F. Salin, "Photodarkening and Photobleaching of an Ytterbium-Doped Silica Double-Clad LMA Fiber," *Optics Express*, Vol. 15, No. 4, 2007, pp. 1606-1611. doi:10.1364/OE.15.001606
- [6] S. Jetschke, S. Unger, U. Ropke and J. Kirchhof, "Photodarkening in Yb Doped Fibers: Experimental Evidence of Equilibrium States Depending on the Pump Power," *Optics Express*, Vol. 15, No. 4, 2007, pp. 14838-14843. doi:10.1364/OE.15.014838
- [7] T. Kitabayashi, M. Ikeda, M. Nakai, T. Sakai, K. Himeno and K. Ohashi, "Population Inversion Factor Dependence of Photodarkening of Yb-Doped Fibers and Its Suppression by Highly Aluminum Doping," *Optical Fiber Communications Conference*, Anaheim, 5 March 2006. doi:10.1109/OFC.2006.215694
- [8] A. D. Guzman Chavez, A. V. Kir'yanov, Y. O. Barmenkov and N. N. Il'ichev, "Reversible Photo-Darkening and Resonant Photo-Bleaching of Ytterbium-Doped Silica Fiber at in-Core 977 nm and 543 nm Irradiation," *Laser Physics Letters*, Vol. 4, No. 10, 2007, pp. 734-739. doi:10.1002/lapl.200710053
- [9] J. Koponen, M. Soderlund, H. J. Hoffman, D. A. V. Kliner, J. P. Koplow and M. Hotoleanu, "Photodarkening Rate in Yb-Doped Silica Fibers," *Applied Optics*, Vol. 47, No. 9, 2008, pp. 1247-1256. doi:10.1364/AO.47.001247
- [10] J. Koponen, M. Laurila and M. Hotoleanu, "Inversion Behavior in Core- and Cladding-Pumped Yb-Doped Fiber Photodarkening Measurements," *Applied Optics*, Vol. 47, No. 9, 2008, pp. 4522-4528. doi:10.1364/AO.47.004522
- [11] S. Yoo, C. Basu, A. J. Boyland, C. Sones, J. Nilsson, J. K. Sahu and D. Payne, "Photodarkening in Yb-Doped Aluminosilicate Fibers Induced by 488 nm Irradiation," *Optics Letters*, Vol. 32, No. 12, 2007, pp. 1626-1628. doi:10.1364/OL.32.001626
- [12] M. Engholm, L. Norin and D. Aberg, "Improved Photodarkening Resistivity in Ytterbium-Doped Fiber Lasers by Cerium Codoping," *Optics Letters*, Vol. 34, No. 8, 2009, pp. 1285-1287. doi:10.1364/OL.34.001285
- [13] M. Engholm, P. Jelger, F. Laurell and L. Norin, "Strong UV Absorption and Visible Luminescence in Ytterbium-Doped Aluminosilicate Glass under UV Excitation," *Optics Letters*, Vol. 32, No. 22, 2007, pp. 3352-3354. doi:10.1364/OL.32.003352
- [14] S. Suzuki, H. A. McKay, X. Peng, L. Fu and L. Dong, "Highly Ytterbium-Doped Silica Fibers with Low Photodarkening," *Optics Express*, Vol. 17, No. 12, 2009, pp. 9924-9932. doi:10.1364/OE.17.009924
- [15] B. P. Fox, Z. V. Schneider, K. Simmons-Potter, W. J. Thomes Jr., D. C. Meister, R. P. Bambha, D. A. V. Kliner and M. J. Soderlund, "Gamma Radiation Effects in Yb-Doped Optical Fiber," *Fiber Lasers IV: Technology, Systems, and Applications, Proceedings of SPIE*, San Jose, Vol. 6453, 22 January 2007, paper 645328, pp. 1-8. doi:10.1117/12.712244
- [16] T. Arai, K. Ichii, S. Tanigawa and M. Fujimaki, "Gamma-Irradiation-Induced Photodarkening in Ytterbium-Doped Silica Glasses," *Fiber Lasers VIII: Technology, Systems, and Applications, Proceedings of SPIE*, San Francisco, 24 January 2011, Vol. 7914, paper 79140K, pp. 1-6.
- [17] N. Groothoff, J. Canning, M. Aslund and S. Jackson, "193 nm Photodarkening of Ytterbium-Doped Optical Fibre," *OSA Meeting on Bragg Gratings, Photosensitivity, and Poling in Glass Waveguides*, Quebec City, 2-6 September 2007, paper BTuC2.
- [18] A. V. Kir'yanov, Yu. O. Barmenkov, I. Lucio Martinez, A. S. Kurkov and E. M. Dianov, "Cooperative Luminescence and Absorption in Ytterbium-Doped Silica Fiber and the Fiber Nonlinear Transmission Coefficient at $\lambda = 980$ nm with a Regard to the Ytterbium Ion-Pairs' Effect," *Optics Express*, Vol. 14, No. 9, 2006, pp. 3981-3992. doi:10.1364/OE.14.006983
- [19] C. G. Carlson, K. E. Keister, P. D. Dragic, A. Croteau, and J. G. Eden, "Photoexcitation of Yb-Doped Aluminosilicate Fibers at 250 nm: Evidence for Excitation Transfer from Oxygen Deficiency Centers to Yb^{3+} ," *Journal of Optical Society of America B*, Vol. 27, No. 10, 2010, pp. 2087-2094. doi:10.1364/JOSAB.27.002087
- [20] Z. Burshtein, Y. Kalisky, S. Z. Levy, P. Le Boulanger and S. Rotman, "Impurity Local Phonon Nonradiative Quenching of Yb Fluorescence in Ytterbium-Doped Silicate Glasses," *IEEE Journal of Quantum Electronics*, Vol. 36, No. 8, 2000, pp. 1000-1007. doi:10.1109/3.853562
- [21] G. Stryganyuk, S. Zazubovich, A. Voloshinovskii, M. Pidzyrilo, G. Zimmerer, R. Peters and K. Petermann, "Charge Transfer Luminescence of Yb^{3+} Ions in LiY1-xYbxP4O12 Phosphates," *Journal of Physics: Condensed Matter*, Vol. 19, No. 47, 2007, Article No. 036202. doi:10.1088/0953-8984/19/3/036202
- [22] S. Girard, Y. Ouerdane, G. Origlio, C. Marcandella, A. Boukenter, N. Richard, J. Baggio, P. Paillet, M. Cannas, J. Bisutti, J.-P. Meunier and R. Boscaino, "Radiation Effects on Silica-Based Preforms and Optical Fibers I: Experimental Study with Canonical Samples," *IEEE Transactions of Nuclear Science*, Vol. 35, No. 5, 2008, pp. 3473-3482. doi:10.1109/TNS.2008.2007297

- [23] M. N. Zervas, F. Ghiringhelli, M. K. Durkin and I. Crowe, "Distribution of Photodarkening-Induced Loss in Yb-Doped Fiber Amplifiers," *Fiber Lasers VIII: Technology, Systems, and Applications, Proceedings of SPIE*, San Francisco, Vol. 7914, 24 January 2011, paper 79140L, pp. 1-8..
- [24] F. Mady, M. Benabdesselam and W. Blanc, "Thermoluminescence Characterization of Traps Involved in the Photodarkening of Ytterbium-Doped Silica Fibers," *Optics Letters*, Vol. 35, No. 21, 2011, pp. 3541-3543. [doi:10.1364/OL.35.003541](https://doi.org/10.1364/OL.35.003541)
- [25] K. E. Mattsson, S. N. Knudsen, B. Cadier and T. Robin, "Photo Darkening in Ytterbium Co-Doped Silica Material," *Fiber Lasers V: Technology, Systems, and Applications, Proceedings of SPIE*, San Jose, Vol. 6873, 21 January 2008, paper 68731C, pp. 1-11. [doi:10.1117/12.763117](https://doi.org/10.1117/12.763117)
- [26] S. Sen, R. Rakhmatullin, R. Gubaydullin and A. Silakov, "A Pulsed EPR Study of Clustering of Yb³⁺ Ions Incorporated in GeO₂ Glass," *Journal of Non-Crystalline Solids*, Vol. 333, No. 1, 2004, pp. 22-27. [doi:10.1016/j.jnoncrysol.2003.09.051](https://doi.org/10.1016/j.jnoncrysol.2003.09.051)
- [27] M. Engholm and L. Norin, "Comment on 'Photo Darkening in Yb-Doped Aluminosilicate Fibers Induced by 488 nm Irradiation'," *Optics Letters*, Vol. 33, No. 11, 2008, pp. 1216-1218. [doi:10.1364/OL.33.001216](https://doi.org/10.1364/OL.33.001216)
- [28] S. Yoo, C. Basu, A. J. Boyland, C. Sones, J. Nilsson, J. K. Sahu and D. Payne, "Reply to Comment on 'Photodarkening in Yb-Doped Aluminosilicate Fibers Induced by 488 nm Irradiation'," *Optics Letters*, Vol. 33, No. 11, 2008, pp. 1217-1218. [doi:10.1364/OL.33.001217](https://doi.org/10.1364/OL.33.001217)
- [29] H. J. Schugar, E. I. Solomon, W. L. Cleveland and L. Goodman, "Simultaneous Pair Electronic Transitions in Yb₂O₃," *Journal of American chemical Society*, Vol. 97, No. 22, 1975, pp. 6442-6450. [doi:10.1021/ja00855a024](https://doi.org/10.1021/ja00855a024)
- [30] F. Auzel and P. Goldner, "Towards Rare-Earth Clustering Control in Doped Glasses," *Optical Materials*, Vol. 16, No. 11, 2001, pp. 93-103. [doi:10.1016/S0925-3467\(00\)00064-1](https://doi.org/10.1016/S0925-3467(00)00064-1)
- [31] A. Lupei and V. Lupei, "RE³⁺ Pairs in Garnets and Sesquioxides," *Optical Materials*, Vol. 24, No. 1-2, 2003, pp. 181-189. [doi:10.1016/S0925-3467\(03\)00123-X](https://doi.org/10.1016/S0925-3467(03)00123-X)
- [32] M. A. Noginov, G. B. Loutts, C. S. Steward, B. D. Lucas, D. Fider, V. Peters, E. Mix and G. Huber, "Spectroscopic Study of Yb Doped Oxide Crystals for Intrinsic Optical Bistability," *Journal of Luminiscence*, Vol. 96, No. 2-4, 2002, pp. 129-140. [doi:10.1016/S0022-2313\(01\)00210-1](https://doi.org/10.1016/S0022-2313(01)00210-1)
- [33] B. Morasse, S. Chatigny, E. Gagnon, C. Hovington, J.-P. Martin and J.-P. de Sandro, "Low Photodarkening Single Cladding Ytterbium Fibre Amplifier," *Fiber Lasers IV: Technology, Systems, and Applications, Proceedings of SPIE*, San Jose, Vol. 6453, 26 January 2009, paper 64530H, pp. 1-8. [doi:10.1117/12.700529](https://doi.org/10.1117/12.700529)
- [34] R. Peretti, A.-M. Jurdyc, B. Jacquier, C. Gonnet, A. Pas-touret, E. Burov and O. Cavani, "How do Traces of Thulium can Explain Photodarkening in Yb-Doped Fibers?," *Optics Express*, Vol. 18, No. 19, 2010, pp. 20455-20460. [doi:10.1364/OE.18.020455](https://doi.org/10.1364/OE.18.020455)
- [35] S. Jetschke, M. Leich, S. Unger, A. Schwuchow and J. Kirchhof, "Influence of Tm- or Er-Codoping on the Photodarkening Kinetics in Yb Fibers," *Optics Express*, Vol. 19, No. 15, 2011, pp. 14473-14478. [doi:10.1364/OE.19.014473](https://doi.org/10.1364/OE.19.014473)
- [36] R. Paschotta, J. Nilsson, P. R. Barber, J. E. Caplen, A. C. Tropper and D. C. Hanna, "Lifetime Quenching in Yb-Doped Fibres," *Optics Communications*, Vol. 136, No. 5-6, 1997, pp. 375-378. [doi:10.1016/S0030-4018\(96\)00720-1](https://doi.org/10.1016/S0030-4018(96)00720-1)
- [37] A. Iho, M. Soderlund, J. J. Montiel i Ponsoda, J. Koponen and S. Honkanen, "Modeling Inversion in an Ytterbium-Doped Fiber," *Optical Components and Materials VI, Proceedings of SPIE*, San Jose, 26 January 2009, paper 721209, pp. 1-8.
- [38] M. P. Hehlen, N. J. Cockroft, T. R. Gosnell and A. J. Bruce, "Spectroscopic Properties of Er and Yb -Doped Soda-Lime Silicate and Aluminosilicate Glasses," *Physical Review*, Vol. 56, No. 15, 1997, pp. 9302-9318. [doi:10.1103/PhysRevB.56.9302](https://doi.org/10.1103/PhysRevB.56.9302)
- [39] V. Peters, "Growth and spectroscopy of Ytterbium-doped sesquioxides," PhD dissertation, Hamburg, 2001.
- [40] P. Barua, E. H. Sekiya, K. Saito and A. J. Ikushima, "Influences of Yb³⁺ Concentration on the Spectroscopic Properties of Silica Glass," *Journal of Non-Crystalline Solids*, Vol. 354, No. 42-44, 2008, pp. 4760-4764. [doi:10.1016/j.jnoncrysol.2008.04.020](https://doi.org/10.1016/j.jnoncrysol.2008.04.020)
- [41] F. Auzel, "A Fundamental Self-Generated Quenching Center for Lanthanide-Doped High-Purity Solids," *Journal of Luminiscence*, Vol. 100, No. 1-4, 2002, pp. 125-130. [doi:10.1016/S0022-2313\(02\)00457-X](https://doi.org/10.1016/S0022-2313(02)00457-X)
- [42] F. Auzel, "Upconversion and Anti-Stokes Processes with f and d Ions in Solids," *Chemicals Review*, Vol. 104, No. 1, 2004, pp. 139-173. [doi:10.1021/cr020357g](https://doi.org/10.1021/cr020357g)
- [43] M. Leich, F. Just, A. Langner, M. Such, G. Schotz, T. Eschrich and S. Grimm, "Highly Efficient Yb-Doped Silica Fibers Prepared by Powder Sinter Technology," *Optics Letters*, Vol. 36, No. 9, 2011, pp. 1557-1559. [doi:10.1364/OL.36.001557](https://doi.org/10.1364/OL.36.001557)